Royal Netherlands
Meteorological Institute
Ministry of Infrastructure and the Environment

Exploring turbulence spectra of Mode-S EHS wind measurements

J. Klip

KNMI Internal Report IR-2014-07

Royal Netherlands
Meteorological Institute
Ministry of Infrastructure and the Environment

TU Delft

Exploring turbulence spectra of Mode-S EHS wind measurements

This report is written as part of the internship of

Joost Klip

at the
Royal Netherlands Meteorological Institute,
Department of Weather Research

Supervisors

Dr. S. de Haan (KNMI)

Ir. J.W. de Vries (KNMI)

Dr. S.R. de Roode (TU Delft)

September, 2014 De Bilt

Preface

This report is part of my internship for my study Applied Physics at TU Delft (Delft University of Technology). In this report the possibility to extract information about turbulence intensity from measurements of commercial aircraft is invesitgated. This research has been performed at KNMI (Royal Netherlands Meteorological institute) during a three month period from May 2014 until July 2014. I would like to thank my supervisor Dr. S. de Haan (Department of weather research, KNMI) for his daily supervision and reviewing my report, he was always there to give advice, provide data and help with practical problems; my co-supervisor Ir. J.W. de Vries (Department of weather research, KNMI) for his help, advice and reviewing my report; Dr. S.R. de Roode (Department of atmosperic physics, TU Delft) for his support and reviewing my report; and further everyone else who contributed to this report. I want to thank KNMI for giving me the opportunity to do this internship. It was a really nice and challenging project. I want to thank all staff members of the department of weather research and in particular my fellow interns for their support and the nice working environment.

Abstract

To improve safety in aviation, it is important that pilots are provided accurate information about turbulence. Therefore research is done to improve turbulence forecasts. To validate those forecasts information about the turbulence intensity is required. This information can be extracted from data obtained via the so called Mode-S Enhanced Surveillance of the air traffic control radar. Via this system a large number of aircraft report their position, their airspeed and their ground speed about every four seconds. From the difference between the ground velocity vector and the air velocity vector the wind vector is calculated. Together with the reported position this provides a method to obtain wind measurement in a rather high resolution. From those wind measurements turbulent kinetic energy spectra are estimated using the periodogram estimator. Those spectra give information about the turbulence intensity. A common problem with the periodogram estimator is that it is quite noisy. In this report a metod is presented to obtain those spectra and to supress the noise. Also it is investigated whether the spectra indeed contain information about turbulence. Main conclusion of this report is that the obtained spectra do contain information about turbulence intensity, but that they are biassed by a noise which is probably dependent on the family the aircraft belongs to and on the average wind speed. It is recommended to investigate the source of the noise, in order to correct for that. Also recommended is to validate the Mode-S EHS data using other measuring methods.

Introduction

Turbulence is a common problem in aviation. It not only causes discomfort for passengers but it can also cause damage to the airplane; injuries to passengers and cabin crew and sometimes even fatalaties. So it is of great importance to identify regions where turbulence is present, to enable pilots to avoid those regions or warn their passengers and cabin crew in time. There are some techological developments, like on board Lidar and X-band radar, to enable pilots to detect turbulence. Non of these methods however are satisfactory when in comes to clear-air turbulence (see Overeem [2002]). Research is done on methods to forecast the presence and intensity of turbulence. In order to validate those forcasts, wind measurements at flight level of the aircraft are required. There are several methods to obtain such wind measurements. One of them is to use data from commercial aircraft. This is done with a radar system called Mode-S EHS that interrogates all aircraft within its range de Haan [2013]. The aircraft are interrogated about every four seconds. They report their position, their air velocity vector and their ground velocity vector. With this information the wind along te flight path can be calculated. To obtain good quality observations, control and calibration of the heading is needed, which reduces the number of observations by a factor 4. Since there are many airplaines interrogated by the system a high resolution wind field can be constructed in this way. This makes this method suitable to obtain a turbulent kinetic energy spectrum in which short length scales are included. Such a spectrum could contain information about the intensity of the turbulence. In this report the possibility will be explored to extract information about turbulence from Mode-S EHS measurements.

0.1 Structure

In the first chapter theory about turbulence is treated and the estimation method for the turbulent kinetic energy spectrum is introduced. The second chapter explains how the wind velocity is obtained from Mode-S EHS data and how the turbulent kinetic energy spectrum is estimated from this wind vector. The third chapter deals with the question wheter the spectra are aircraft independent; the spectra are compared to a theoretical result and and it is investigated whether on a stormy day the spectrum shows more signal than on a calm day. The fourth chapter contains the conclusion and recommendations for further research.

Contents

Chapter 1

Theory

1.1 Governing equations of fluid flow

In general fluid flow is described by the continuity equation and the Navier-Stokes eqautions. In atmospheric flows the density ρ and the kinematic viscosity ν are in good approximation constant so that those equations read:

$$\frac{\partial u_i}{\partial x_i} = 0 \tag{1.1a}$$

$$\frac{\partial u_i}{\partial t} + \frac{\partial u_i u_j}{\partial x_j} = -\frac{1}{\rho}\frac{\partial p}{\partial x_i} + \nu\frac{\partial^2 u_i}{\partial x_j^2}. \tag{1.1b}$$

Here u_i is the i-th component of the wind. Note that Einstein‘s summation convention is used. In the case of turbulent flow there is no analytical solution known to this set of equations. Using Reynolds decomposition it is however possible obtain information about the flow without solving those equations. The idea is to write all variables as a sum of a mean value and a deviation from that mean. So for example $\psi = \overline{\psi} + \psi'$ where $\overline{\psi}$ denotes the mean value of ψ and ψ' denotes the deviation from de mean of ψ. More details about Reynolds decomposition can be found in Pope [2011]. Using Reynolds decomposition equations (1.1) can be rewritten as

$$\frac{\partial \overline{u_i}}{\partial x_i} = 0 \tag{1.2a}$$

$$\frac{\partial \overline{u_i}}{\partial t} + \overline{u_j}\frac{\partial \overline{u_i}}{\partial x_j} = -\frac{1}{\rho}\frac{\partial \overline{p}}{\partial x_i} + \nu\frac{\partial^2 \overline{u_i}}{\partial x_j^2} - \frac{\partial \overline{u_i' u_j'}}{\partial x_j}. \tag{1.2b}$$

In this way it is also possible to get an expression for the kinetic energy per unit of mass contained in the flow. The kinetic energy per unit mass inside a flow is given by:

$$E = \frac{1}{2}u_i u_i. \tag{1.3}$$

Averaging equation (1.3) yields:

$$\overline{E} = \frac{1}{2}\overline{u_i}\,\overline{u_i} + \frac{1}{2}\overline{u_i' u_i'}. \tag{1.4}$$

In 1.4 the first term on the right hand side is the kinetic energy contained in the mean flow, the last term is the average kinetic energy of the turbulent fluctuations. This quantity is often referred to as the turbulent kinetic energy, and is denoted by k.

1.2 Autocorrelation and the turbulent kinetic energy

The two-point correlation function of u_i' and u_j' is defined as

$$R_{ij}(\vec{x},\vec{x}+\vec{d},t) = \overline{u_i'(\vec{x},t)\,u_j'(\vec{x}+\vec{d},t)} \tag{1.5}$$

Here $\vec{x} = (x,y,z)$ and $\vec{d}$ is a 3-d displacement vector. So the two point correlation function is in principle a function of 3-d space and time. The measurements used in this investigation are taken at a more or less constant flight level of the airplane, so that z can be assumed to be constant. Furthermore the turbulence is assumed to be statistically homogeneous in the x and y directions and statistically stationary. Homogeneity implies that the two point correlation function is dependent on the displacement $\vec{d}$ and not on x and y. Stationarity implies that the correlation function is time independent. Also because of homogeneity we can choose the ground trajectory as x-axis if it is not too curved. This means that the two point correlation function can be written as:

$$R_{ij}(d) = \overline{u_i'(x)\,u_j'(x+d)} \tag{1.6}$$

A special type of the two point correlation function is the autocorrelation. The autocorrelation is the two point correlation of a signal with itself, so for turbulence which is statistically stationary and statistically homogeneous the autocorrelation of the x-component of the velocity fluctuations $u_1'(\vec{x},t)$ reads:

$$R_{11}(d) = \overline{u_1'(x)\,u_1'(x+d)} \tag{1.7}$$

For zero displacement we get $R_{11}(r=0) = \overline{u_1'u_1'}$. So the turbulent kinetic energy can be written as:

$$k = \frac{1}{2}\left(\overline{u_1'^2} + \overline{u_2'^2} + \overline{u_3'^2}\right) = \frac{1}{2}R_{ii}(0) \tag{1.8}$$

$R_{ii}(d)$ can also be written as the Fourier transform of a function $\Phi_{ii}(\kappa)$:

$$R_{ii}(d) = \int_{-\infty}^{\infty} \Phi_{ii}(\kappa)e^{i\kappa d}\,\mathrm{d}\kappa \tag{1.9}$$

Obviously:

$$k = \int_{-\infty}^{\infty} \frac{1}{2}\Phi_{ii}(\kappa)\,\mathrm{d}\kappa \tag{1.10}$$

Here κ is the wavenumber. So $\frac{1}{2}\Phi_{ii}(\kappa)$ can be seen as the spectral energy density function. Via the inverse Fourier transform we get:

$$\Phi_{ii}(\kappa) = \frac{1}{2\pi}\int_{-\infty}^{\infty} R_{ii}(r)e^{-i\kappa d}\,\mathrm{d}r \tag{1.11}$$

Recalling that $R_{ii}(d) = \overline{u_i'u_i'}$. We can write that:

$$R_{ii}(d) = \frac{1}{N}\sum_{n=0}^{N-1} u_i'(x)u_i'(x+d_n), \quad N\to\infty, \quad d_n = n\Delta d \tag{1.12}$$

1.3 A brief introduction into turbulence

In section 1.1 we have seen that a turbulent flow field can be decomposed into a mean part an a fluctuating part. It is clear that the fluctuations are instationary and highly irregular. Nevertheless the fluctuations can be described qualitatively as a collection of eddies with a wide variety of length scales and velocity scales. The largest eddies have a typical length scale l_0 which is of the order of the length scale of the flow and a typical velocity scale u_0 which is of the order of the mean flow velocity. This means that they have a Reynolds number ($Re_0 = u_0 l_0/\nu$) of the order of the Reynolds number of the flow, here ν is the kinematic viscosity. So in those eddies viscous effects are negligible. The large eddies are unstable, they break up into smaller eddies, which will also break up. This will go on until the Reynolds number is so low that viscous effects start to play a role and the eddies are dissipated by viscosity. This mechanism was introduced by Richardson [1922] is known as the Richardson energy cascade. So the dissipation of energy happens at the end of a sequence of processes, so the dissipation rate ϵ is determined by the first process in the sequence which is the transfer of energy from the largest eddies. Given that the lifetime of those eddies can be estimated as $\tau_0 = l_0/u_0$ and that their energy is of the order of u_0^2 so that the rate of energy transfer can be supposed to scale with $u_0^2/\tau_0 = u_0^3/l_0$. Kolmogorov [1941] presented a way to estimate the length, velocity and time scales of the smallest eddies, based on two hypotheses:

Kolmogorov's hypothesis of local isotropy. At sufficiently high Reynolds number, the small-scale turbulent motions ($l \ll l_0$) are statistically isotropic.

Kolmogorov's first similarity hypothesis. In every turbulent flow at sufficiently high Reynolds number, the statistics of the small-scale motions have a universal form that is uniquely determined by ν and ϵ.

Using those hypotheses Kolmogorov found that the length, velocity and time scales of the smallest eddies are determined by:

$$\eta = \left(\nu^3/\epsilon\right)^{1/4}, \tag{1.13}$$

$$u_\eta = (\epsilon\nu)^{1/4}, \tag{1.14}$$

$$\tau_\eta = (\nu/\epsilon)^{1/2}. \tag{1.15}$$

These are known as the Kolmogorov scales. The turbulence spectrum can be devided into three different ranges, as can be seen in 1.1.
The inertial subrange, where length scales are in the range of $l_0 \ll l \ll \eta$, is of special interest because in this range Kolmogorov obtained the universal form of the turbulent kinetic energy spectrum. To this end he formulated a third hypothesis:

Kolmogorov's second similarity hypothesis. In every turbulent flow at sufficiently high Reynolds number, the statistics of the motions of scale l in the range of $l_0 \ll l \ll \eta$ have a universal form that is uniquely determined by ϵ independent of ν.

Based on the three hypotheses mentioned above Kolmogorov deduced that the spectral energy density in the inertial subrange must be proportional to $\kappa^{-5/3}$. In figure 1.1 it can be seen that the spectrum in the inertial subrange lies on a straight line.

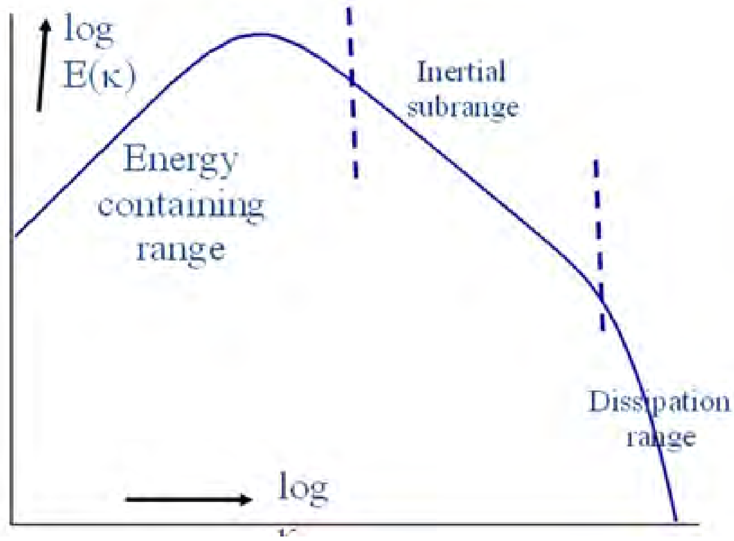

Figure 1.1: Classification of the length scales in the energy cascade with in the inertial subrange the Kolmogorov's -5/3 spectrum (taken from Moreno [2010])

The slope of this line has to be $-5/3$ according to the Kolmogorov theory (since the axis have logarithmic scales the function $E(\kappa) = C\kappa^{-5/3}$ is displayed as a straight line with slope $-5/3$).

1.4 Estimation

In section 1.2 the spectral energy density function has been introduced. In this section we will see how this function can be estimated using a sequence of samples of the wind velocity. Suppose we have a sequence of measured velocity values $\{\vec{u}(r_1)', \vec{u}(r_2)'....\vec{u}(r_N)'\}$ where $r_j = j\Delta r$. A possible way to estimate the autocorrelation is (assuming $\Delta r = 1$km):

$$\hat{R}_{ii}(k) = \frac{1}{N}\sum_{j=k}^{N-1} u_i'(r_j)u_i'(r_j - k) \tag{1.16}$$

There are also other possibilities to estimate the autocorrelation function, but for this one it is guaranteed that its Fourier transform is nonnegative for all frequencies (P. van den Hof [2006]). A natural way to estimate Φ_{ii} is to take the Discrete Fourier Transform (DFT) of $\hat{R}_{ii}$. According to P. van den Hof [2006] this gives:

$$\hat{\Phi}_{ii}(\kappa) = \frac{1}{N}|U_N(\kappa)|^2 \tag{1.17}$$

This $\hat{\Phi}_{ii}$ is called the periodogram estimator and $U_N(\kappa) = \text{DFT}(u_i'(r_j))$.

Chapter 2

Data processing

2.1 Wind measurements

All aircraft have equipment to measure the speed of the aircraft relative to the air (v_a); its heading angle with respect to the north (α) and its position. Almost all of them transmit those measurements to the Air Traffic Control when interrogated by a called Mode-S EHS (the selective mode of the enhanced surveillance radar). A method to derive wind information from these measurements is presented in de Haan [2013]. This method uses the velocity of the aircraft relative to the air ($\vec{v}_a$), which is determined by v_a and α, and its velocity relative to the ground ($\vec{v}_g$), given by the ground speed (v_g) and the track angle (α_g). The wind velocity is then simply the difference between $\vec{v}_g$ and $\vec{v}_a$:

$$\vec{u} = \vec{v}_g - \vec{v}_a \tag{2.1}$$

The data mentioned above are obtained by Air Traffic Control using a radar signal to interrogate all aircraft separately every radar sweep. An aircraft with Mode-S EHS equipment will respond sending the data over a radio link towards the ground. Since the aircraft report their position, the thus obtained wind velocity can be expressed as a function of position. The position is reported as latitude (θ) and longitude (ϕ) coordinates. For convenience those are converted to Cartesian coordinates using a equidistant projection centered around $\theta = 50°, \phi = 8°$

2.2 Estimating the spectrum

To get an estimate of the spectral energy density function the wind measurements are expressed as a function of the path length r_n along the flight path. The path length is calculated as:

$$r_1 = 0, \qquad r_i = \sum_{i=1}^{n-1} (x_{i+1} - x_i)^2 + (y_{i+1} - y_i)^2, \qquad n \geq 2. \tag{2.2}$$

From $u(r_i)$ we have to obtain the fluctuating part $u'(r_i)$, so we have to estimate the mean flow somehow. Furthermore the largest structures in atmospheric flows may be larger than the length of the flights. This can cause the data to have a linear trend which introduces a κ^{-2} contribution to the spectrum. An effective method to get rid of the length scales larger than the sample length (and the mean), is to subtract a linear function $\overline{u}$, such that $u(0) - \overline{u}(0) = u(r_{n-1}) - \overline{u}(r_{n-1}) = 0$ Vogelzang [2013]. So we assume $u'(r_i)$ to be given by:

$$u'(r_i) = u(r_i) - \frac{\Big(u(r_{n-1}) - u(0)\Big) r_i + u(0) r_{n-1}}{r_{n-1}} \tag{2.3}$$

With $u'(r_n)$ known it is possible to construct a periodogram provided the values of r_n are equispaced. This is in general not the case because data of several radars are combined. Those radars can have different sweep periods and they generally operate out of phase. To overcome this problem the data has been resampled, with sampling frequency f_s, onto a regularly spaced grid, using linear interpolation between consecutive points. Another problem commonly encountered with the periodogram is that it has quite a lot of variance. There is a method to reduce the variance. Suppose we have a sequence of N data points. This sequence can be divided into m subsequences of length N/m (if $\mathrm{N/m} \in \mathbb{N}$). From each of those subsequences a periodogram is made and those periodograms are averaged. There are two major drawbacks of this procedure. The first one is that periodograms of shorter sequences suffer more from spectral leakage. The other is that the maximal turbulence length scale that can be observed is equal to the length of the line segments considered. In other words: by taking shorter sequences the maximal wavelength that can occur in the periodogram gets shorter. A second way to reduce the variance is taking the average of the periodograms obtained from several flights. In this investigation both strategies will be combined. So each flight will be divided into sequences of N data points; of each sequence a periodogram will be made and finally the average of the thus obtained periodograms will be taken.

Chapter 3

Results

In this chapter the obtained spectra will be compared to the Kolmogorov spectrum; differences between aircraft types will be shown and the difference between a calm day and a stormy day will be shown.

3.1 Comparison of different aircraft types

In this section it will be checked whether the measurements of the wind field are independent of the aircraft type. This is expected to be the case because the wind field itself is obviously independent of the aircraft type. On the other hand there is a possibility that errors in the measurement of the airspeed occur, for instance due to usage of different types instruments in different aircraft types or an aircraft specific flow pattern around the measurement device that induces a bias. If the measurements are aircraft dependent there must be differences in the spectra obtained by different aircraft.

3.1.1 Comparison of aircraft within the same family

In this subsection Boeing 737-800's (B738's) are compared to Boeing 737-700's (B737's) since these aircraft types are part of the same family, and thus similar, it is even less likely that their spectra exhibit differences due to aircraft specific noise.

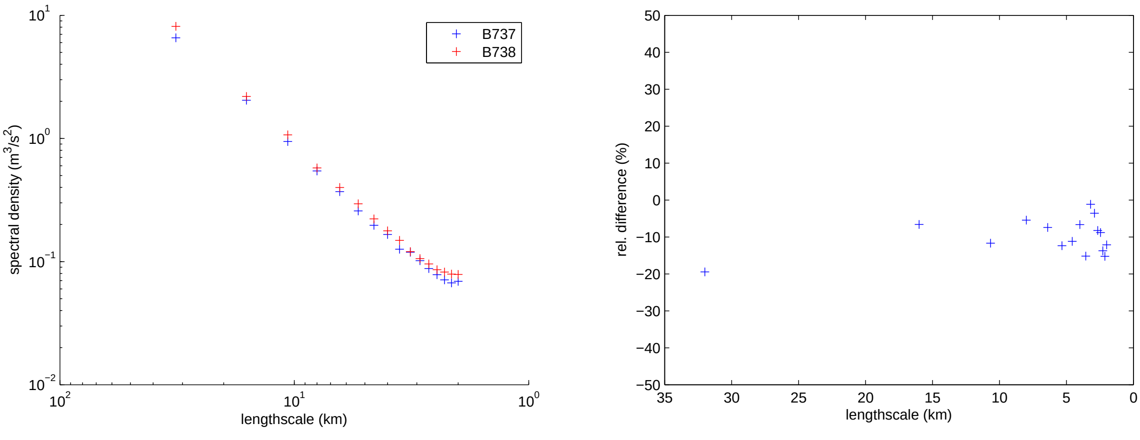

(a) The spectrum of B737's (blue) and B738's (red). (b) The relative difference between the spectra.

Figure 3.1: comparison of the spectra of B737's and B738's, $f_s = 1\text{km}^{-1}$ and $N = 32$.

Figure 3.1 shows the spectra of the two aircraft types and the relative difference, calculated as $\frac{\hat{\Phi}_{ii,B737}-\hat{\Phi}_{ii,B738}}{\hat{\Phi}_{ii,B738}} * 100\%$, between the two. This figure shows that the B737's measure structurally less power than B738's. Especially in figure 3.1b we see that the spectrum of the B737's lies on average about 10% lower than that of the B738's. The spectra in figure 3.1 are obtained from flights in quite a large area as can be seen in figure 3.2. Also it can be seen that there are areas wehere one aircraft type is relatively stronger represented than the other one. So the differences in the spectrum could also occur due to regional differences in turbulence intensity. To investigate this we will zoom in on an area of radius 200km. The flights in this area are shown in figure 3.3

Figure 3.2: Flights of B737's (black) and B738's (red) used to construct figure 3.1.

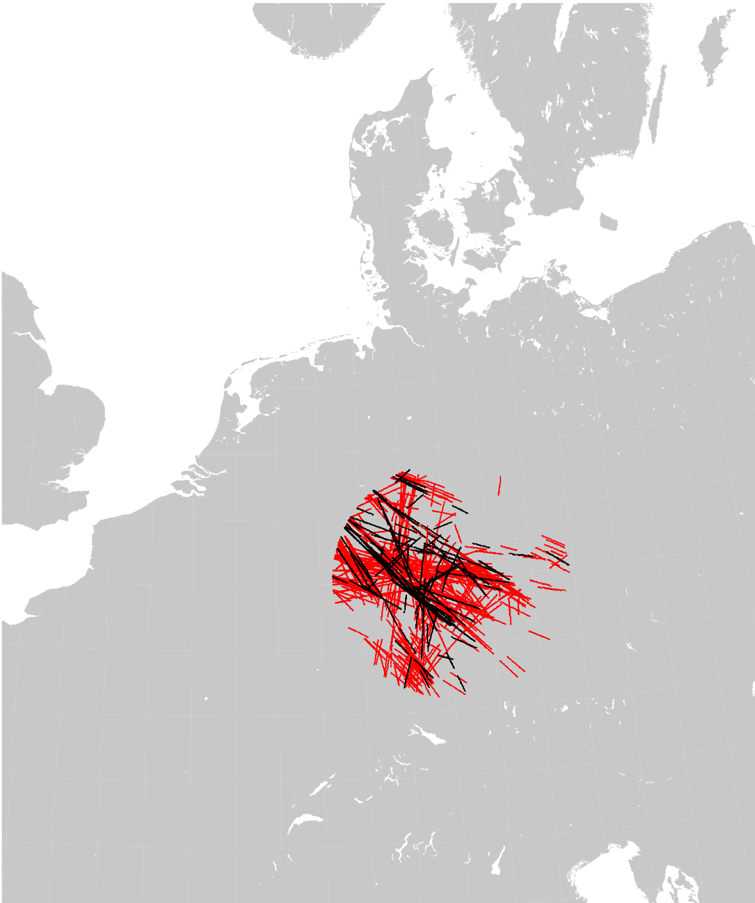

Figure 3.3: Flights of B737's (black) and B738's (red) in a region of 200km radius.

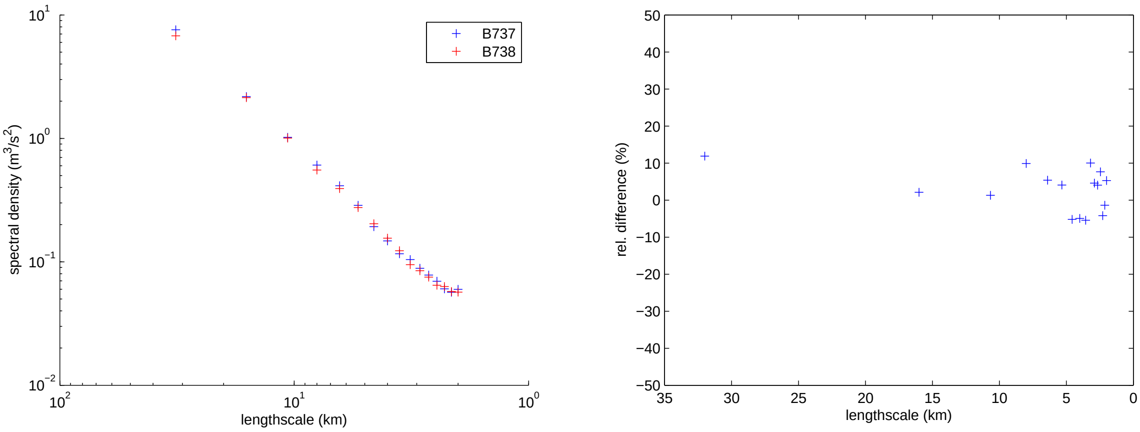

(a) The spectrum of B737's (blue) and B738's (red). (b) The relative difference between the spectra.

Figure 3.4: comparison of the spectra of B737's and B738's in the region given in figure 3.3, $f_s = 1\text{km}^{-1}$ and $N = 32$.

.

Figure 3.4 shows the spectra of the aircraft in the selected area. In figure 3.4b it can be seen that on average there is no difference between the spectra anymore. This implies that the differences found in figure 3.1 are not caused by differences specific for the aircraft type. Further study showed that the spectra seem sensitive to the location of measurement. In figure 3.5 we see that when another region is selected the B737's suddenly measure structurally more power than the B738's. Why the measurements are so sensitive to changes of the measurement region is not clear. A possible explanation is the presence of the a trough above the Netherlands (figure 3.6). Such a trough is known to cause turbulence. It is possible that the B737's are more strongly present in the proximity of the trough than the B738's. This would mean that the B737's on average measure more power. If this is the case an even smaller area of measurement should be considered, but when doing this the results get noisy so it gets harder to draw conlusions. Another explanation would be that individual aircraft of the same type differ from each other, for example due to differences in their sensors, though this explanation is less plausible since the spectra presented here are constructed using 34 individual aircraft or more.

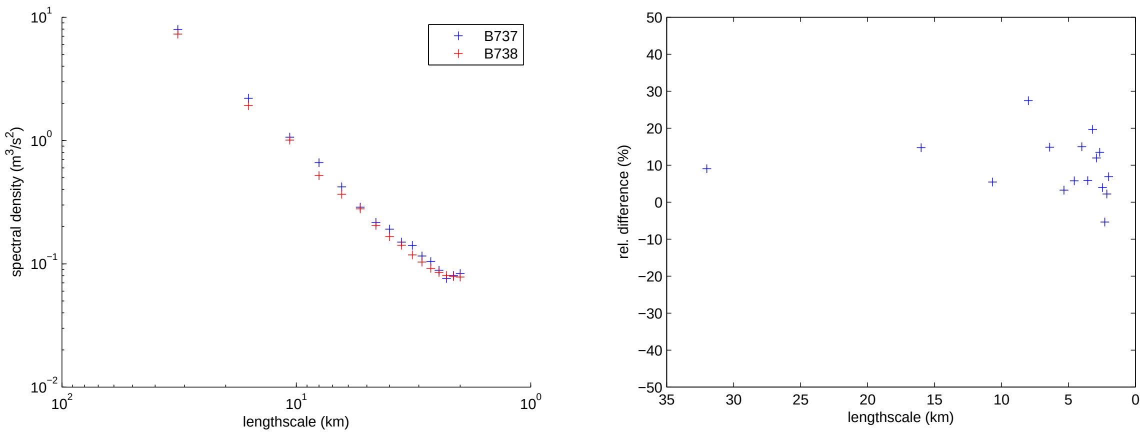

(a) The spectrum of B737's (blue) and B738's (red). (b) The relative difference between the spectra.

Figure 3.5: comparison of the spectra of B737's and B738's, obtained in a region of 200km radius, shifted 150km to the west and 250km to the north compared to the region given in figure 3.3, $f_s = 1\text{km}^{-1}$ and $N = 32$.

.

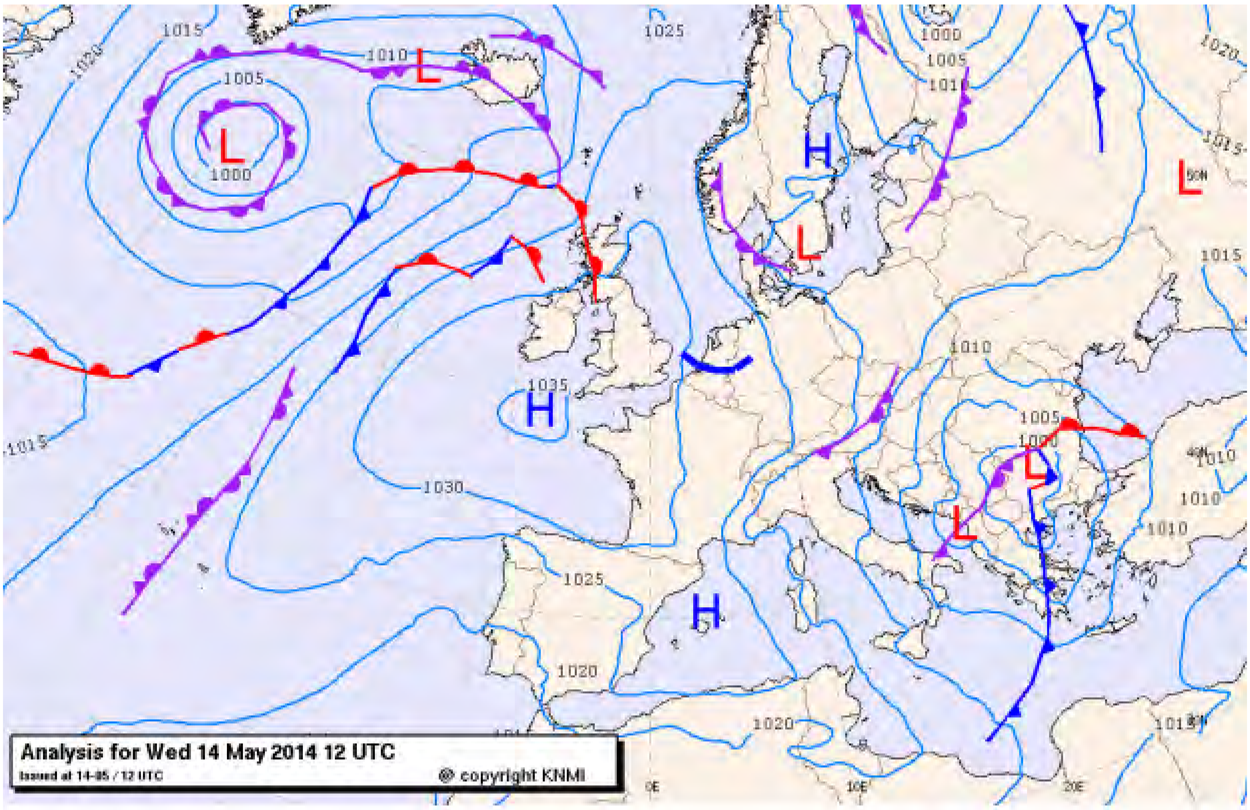

Figure 3.6: The weather situation on May 14th 2014 at 12 UTC

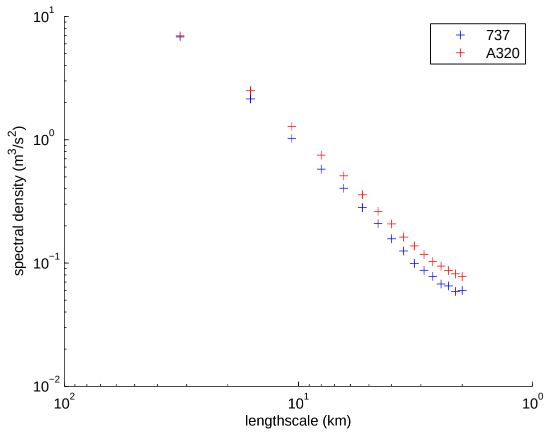

(a) The spectrum of 737's (blue) and A320's (red).

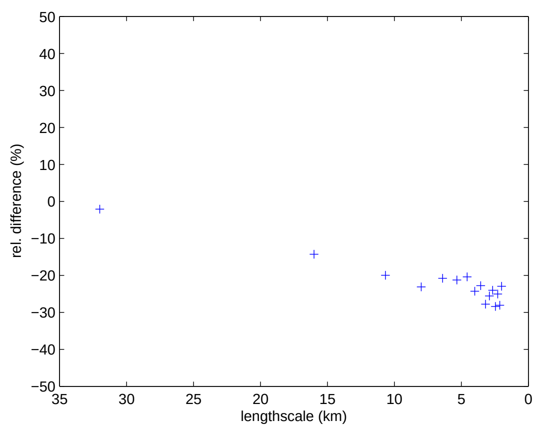

(b) The relative difference between the spectra.

Figure 3.7: comparison of the spectra of 737's and A320's, obtained in the region given in figure 3.3, $f_s = 1\text{km}^{-1}$ and $N = 32$

3.1.2 Intercomparison of different families of aircraft

In section 3.1.1 we have seen that the measurements are quite sensitive to the location. This makes it difficult to determine whether differences in the measurements of aircraft types are caused by a bias specific for the aircraft type or by something else such as difference in atmospheric circumstances. Despite these difficulties in this subsection an attempt is made to find out whether there are structural differences between families of aircraft. To do so it is assumed that there are no aircraft specific differences in the measurements between the aircraft types within a family. In this way also families of which relatively few flights are available can be used. First we will look at the differences between two families with aircraft of comparable mass, namely Boeing 737's (737's) and Airbus A320's (A320's). In figure 3.7 it can be seen that at the short length scales the A320's measure more power than the 737's but as the lengthscales get longer the power of the 737's increases faster. Although in this case also the dependence on the location of measurement shows up the 737's measure a steeper spectrum and significantly less power for the short length scales than the A320's for every location of measurement. So there seem to be differences in the measurements of these aircraft due to differences specific for the family they belong to. These differences in slope could not be revealed when comparing one of those families to others, because of the other families to few flights were available to get enough noise reduction.

3.2 Comparison to the Kolmogorov spectrum

To verify that the obtained spectrum is the spectrum of a turbulent wind field the obtained spectra will be compared to the Kolmogorov spectrum. In the previous section we have seen that the slope of the spectrum can vary between the varous aircraft families. Therefore four families, the A320's, the 737's the Embraer Jets (ERJ's) and the Boeing 777's (777's), will be examined in this section. In figure 3.8 the spectra of the four families are given together with the line $\kappa^{-5/3}$ from the Kolmogorov spectrum. As can be seen all spectra lie more or less on a straight line except at the very smallest length scale where all of the spectra flatten. This overestimation of the spectral density occurs due to aliasing. Apart from the aliasing effect the spectrum of the A320's is almost the same as the Kolmogorov spectrum. Like we saw before the spectrum of the 737's is a bit steeper. The spectra of the other two families are a bit noisier, because less flights were available. Nevertheless it can be seen that the spectrum of the ERJ's is close to the Kolmogorov spectrum and that the spectrum of the 777's is somewhat steeper. So every family of aircraft seems to have a spectrum with a specific slope. Since all of the measured spectra do not deviate very much from the Kolmogorov spectrum the measurements probably consist of isotropic turbulence, to a greater or lesser extend disturbed by a noise specific for the family of aircraft. It is hard to tell what is the cause of this noise. When looking at the size of the different aircraft, the A320's and the 737's are mostly comparable, the ERJ's are a bit smaller and the 777's are much larger. In the spectra however the biggest difference occurs between the A320's and the 737's. So the noise is not dependent on the size of the aircraft.

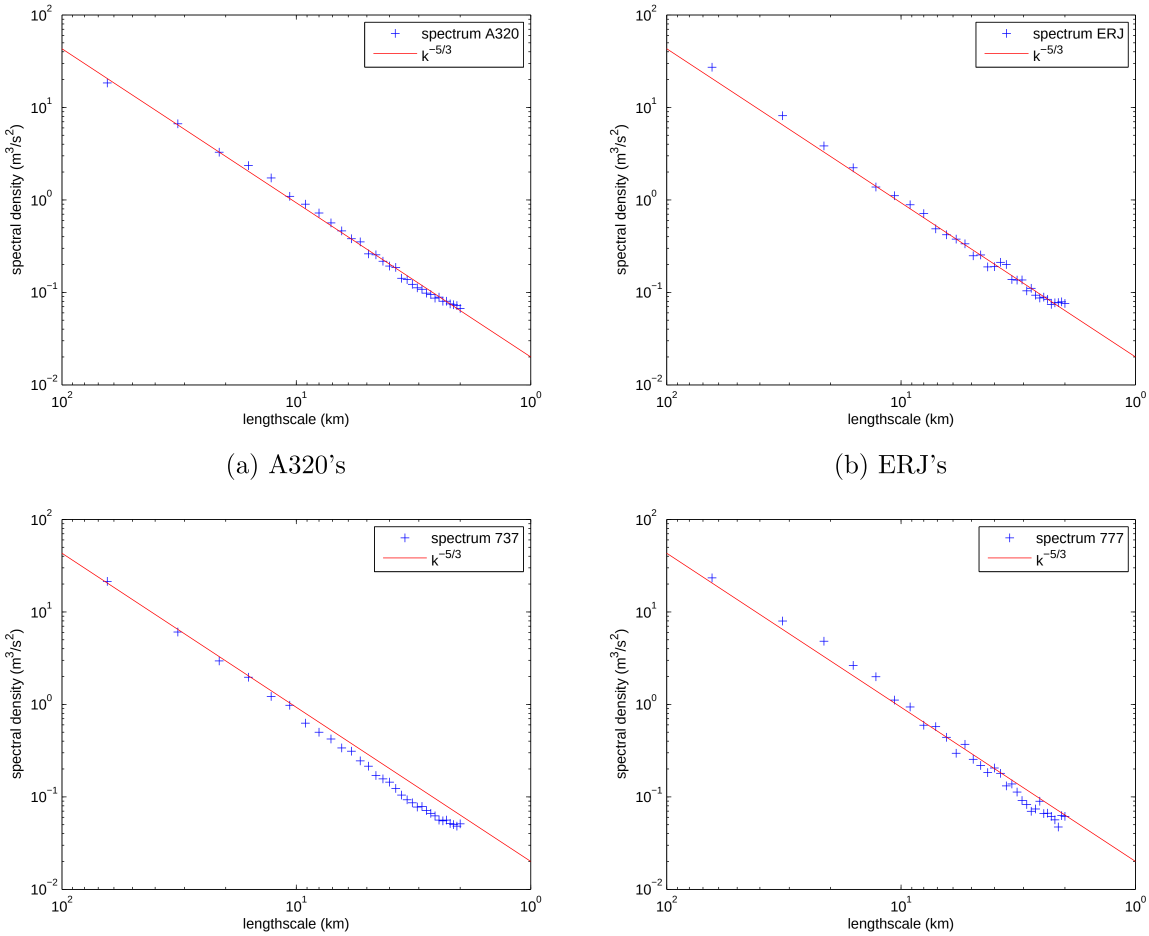

(a) A320's (b) ERJ's

(c) 737's (d) 777's

Figure 3.8: Comparison of the spectra of four families of aircraft to the Kolmogorov spectrum, $f_s = 1\text{km}^{-1}$ and $N = 64$

3.3 Calm weather vs stormy weather

During storm more turbulence is expected to be present in the atmosphere. In this section it will be investigated whether it is possible to distiguish a stormy day from a calm day. This will be done by comparing the spectra of A320's on May 14th 2014 with the spectra of A320's on December 5th 2013. The weather situation on both day are displayed in figures 3.6 and 3.10 respectively. In figure 3.11 the flights used to construct the spectra are displayed. As can be seen the area of measurement was highly affected by the storm. On December 5th 2013 1 hour averaged wind speeds of up to 25m/s with gusts of up to 38m/s were measured inside this area,[1] while May 14th 2014 was a day with calm high pressure weater. In figure 3.9 it can be clearly seen that the airplanes measure significantly more power during the storm, when compared to the calm day. This is in accordance with our expectations and is a clear indication that turbulence intensity can be measured using this method. Another observation that can be made is that the slope of the spectrum during the storm is steeper than the slope of the spectrum of the calm day. So the magnitude of the bias in the measurements seems to be dependent on the intensity of the turbulence and/or on the average windspeed.

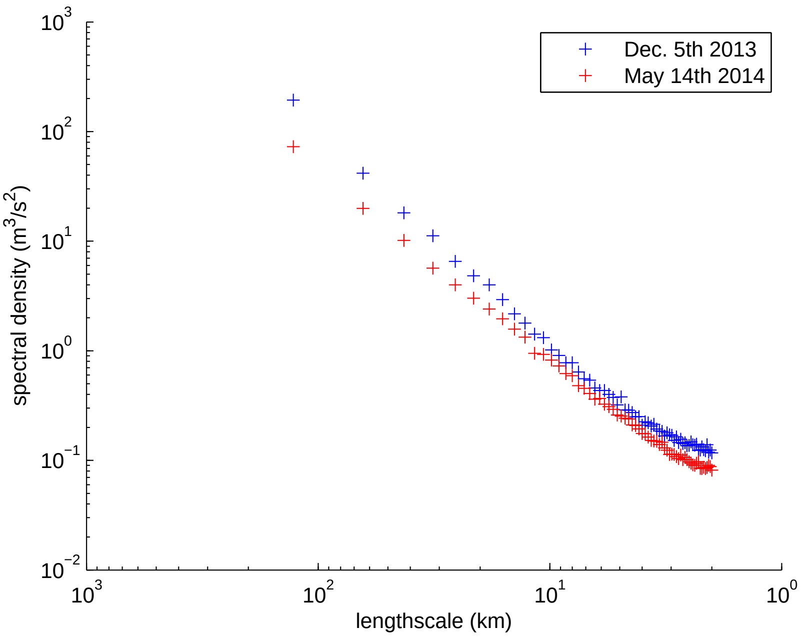

Figure 3.9: Comparison between the spectra of A320's measured on May 14th 2014 and on December 5th 2013, $f_s = 1\text{km}^{-1}$ and $N = 128$

[1]Source: http://www.knmi.nl/klimatologie/storm_dec13.html

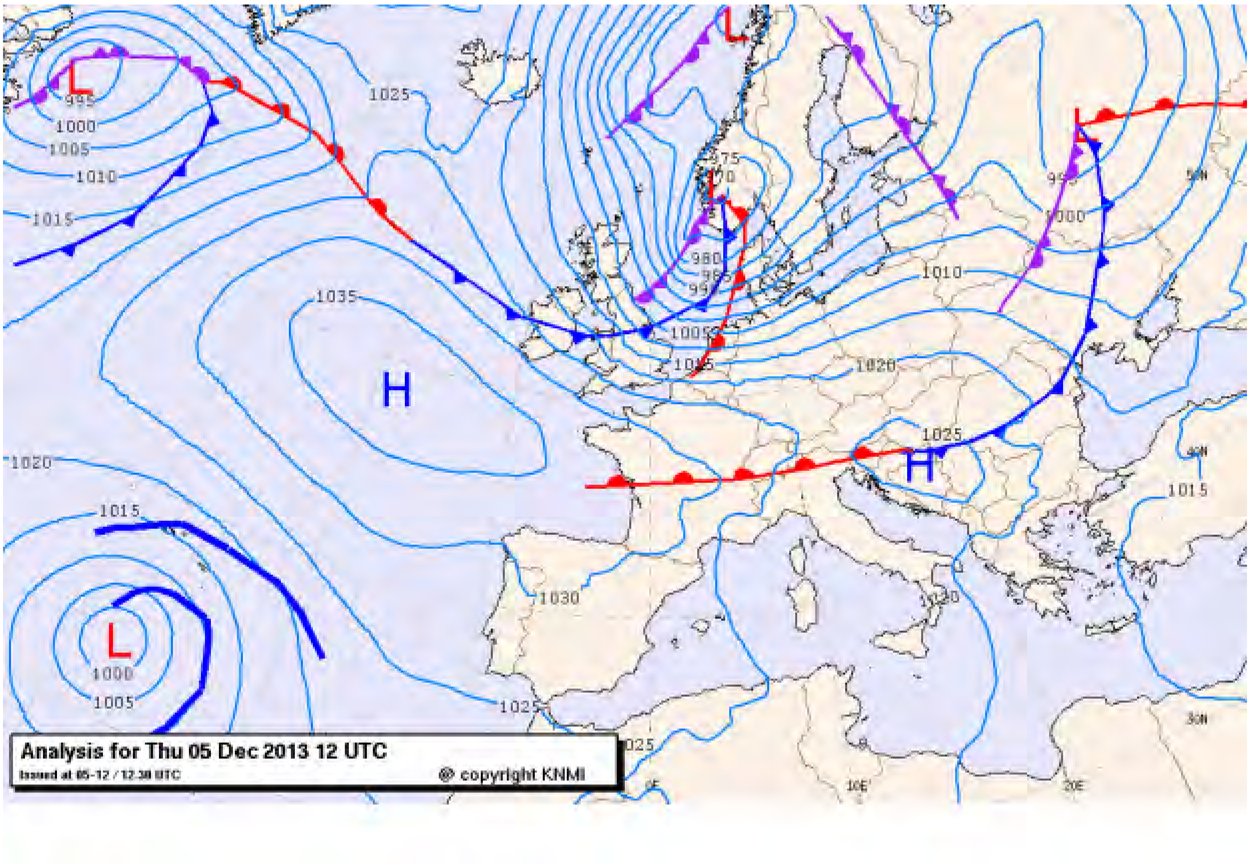

Figure 3.10: The weather situation on December 05th 2013 at 12 UTC

Figure 3.11: Flights of A320's on December 5th 2013 (black) and on May 14th 2014 (red) in a region of 200km radius.

Chapter 4

Conclusion and recommendations

At first sight the spectra obtained from the Mode-S EHS winds seem to exhibit quite a lot of differences from aircraft type to aircraft type, even between aircraft types with minor differences (like members of the same family). When taking a closer look at this it turned out that the differences were probably caused by regional differences in turbulence intensity. When looking at a smaller region the spectra were shown to be dependent on the location of this region. A possible explanation for this is that weather systems, such as troughs, present inside the region locally cause stronger turbulence and that one of the aircraft types considered is represented more strongly in the proximity of such a weather system. So between the spectra of the different aircraft within one family there seem to be no structural differences.
When comparing families of aircraft structural differences occur. It has been shown that the spectra of some of the aircraft families coincide with the Kolmogorov spectrum, while others follow a somewhat steeper line. This suggests that the measurement of the airspeed is biased by a non-white noise which is specific for the aircraft family considered. Also it has been shown that the slope of the spectrum depends on the wind speed, so this noise appears to be dependent on the wind speed. Lastly the comparison between the calm day and the stormy day clearly show that during the stormy day more turbulence is measured than during the calm day. This shows that the Mode-S EHS data have the potential to reveal areas where turbulence is present.

Further research can be conducted to the nature of the noise in the measurement of the airspeed. Since this noise extends over a wide variety of length scales much larger than the aircraft itself, it seems not likely that the noise is caused by a specific flow pattern around the measurement device. The noise could be caused by inertia of the measurement device, which acts as a high pass filter. Another interesting topic would be to compare the spectra obtained from the Mode-S EHS data to wind spectra obtained from other measurement methods such as radar, in order to validate the Mode-S EHS data.
Furthermore the reason behind the regional differences found when comparing similar airplaines can be investigated further. Especially the question whether these differences occur due to the proximity some weather system or due to an aircraft specific cause. Another problem that occured is that in order to properly suppress the noise from the periodogram estimator a lot of samples are required. The noise could be supressed by multiplying the samples with a window function before applying the FFT. This however causes a bias. So here an optimum has to be found between good noise reduction without causing too much bias.

Summarizing the recommendations:

- Research on the nature of the noise in the airspeed.
- Validation of the Mode-S spectra using spectra from other measurement methods.
- Investigation of the regional differences.
- Trying to suppress the noise using window functions, without introducing much bias.

Bibliography

S. de Haan. An improved correction method for high quality wind and temperature observations derived from Mode-S EHS, 2013.

A.N. Kolmogorov. The local structure of turbulence in incompressible viscous fluid for very large Reynolds number. *Dokl. Akad. Nauk SSSR*, 30:299–303, 1941.

C.G. Moreno. Turbulence, vibrations, noise and fluid instabilities. practical approach., 2010. URL `http://www.intechopen.com/books/computational-fluid-dynamics/turbulence-vibrations-`

A. Overeem. Verification of clear-air turbulence forecasts, 2002.

A. den Dekker P. van den Hof. Signal analysis and estimation. Lecture notes Delft University of Technology, 2006.

S.B. Pope. *Turbulent Flows*. Cambridge University Press, 2011.

L.F. Richardson. *Weather Prediction by Numerical Process*. Cambridge University Press, 1922.

J. Vogelzang. How to calculate wind spectra, 2013. URL `http://nwpsaf.eu/deliverables/scatterometer/nwpsaf-kn-tr-008_howtocalculatewindspectra.pdf`.

A complete list of all KNMI-publications (1854 – present) can be found on our website

www.knmi.nl/knmi-library/knmipub_en.html

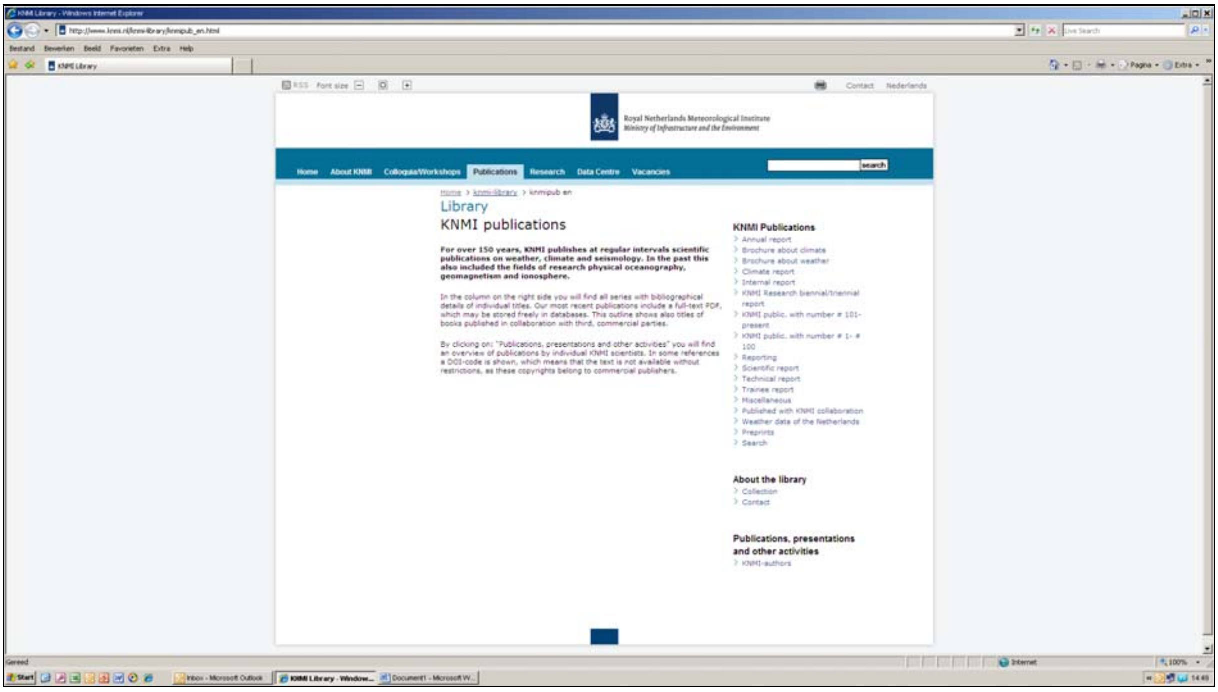

The most recent reports are available as a PDF on this site.